Medical Engineering and Physics 66 (2019) 18–25

Contents lists available at ScienceDirect

Medical Engineering and Physics

journal homepage: www.elsevier.com/locate/medengphy

Dynamic analysis of varus knee using a subject-specific multibody model of the knee before and after osteotomy

Fateme Badie, Hamid Reza Katouzian*, Mostafa Rostami

Biomechanics and Sport Engineering Group, Biomedical Engineering Department, Amirkabir University of Technology, Hafez Ave., Tehran, Iran

ARTICLE INFO

Article history:
Received 27 August 2017
Revised 27 January 2019
Accepted 1 February 2019

Keywords:
Knee
Osteotomy
Multibody model
Finite element model
Dynamic analysis

ABSTRACT

Varus misalignment of the hip-knee-ankle angle causes greater loads on the medial compartment of the knee and increases the risk of developing knee osteoarthritis. High tibial osteotomy is a surgical method where the load-bearing axis is shifted laterally. The purpose of this study is to define a subject-specific three-dimensional multibody model of the knee to investigate the effect of osteotomy on cartilages and menisci during the stance phase of gait. It is assumed that osteotomy transfers load-bearing to the lateral parts of the knee. Magnetic resonance images of a patient with varus alignment were used to generate the geometries of the bones, cartilages, and menisci. Then, an experimental approach was used to determine the parameters for the stiffness matrices and compliant contact models of the tibio-meniscofemoral articulations with the use of finite element solutions. As indicated by the research findings, the contact force at the medial cartilage decreased as the load-bearing axis was transferred to the lateral parts. This subject-specific noninvasive analysis of contact force can be considered as a preoperative assessment tool for the surgeon. to predict the effects of high tibial osteotomy and the shifting of the load-bearing axis to the soft tissues of the knee.

© 2019 Published by Elsevier Ltd on behalf of IPEM.

1. Introduction

Varus knee is a misalignment of the hip-knee-ankle angle that is less than 180°; the normal knee angle is between 178° and 180° [1]. Gait analysis indicates that varus knee alignment increases knee adduction moments and knee flexion, which results in greater quadriceps tension resisting knee flexion. The higher the quadriceps tension, the greater the joint force. Therefore, varus alignment of the knee and, consequently, the higher loads on the medial compartment develop the risk for osteoarthritis (OA) [2].

High tibial osteotomy (HTO) is a widely performed surgical procedure that is used to address medial knee arthritis. The goals of HTO are to reduce knee pain by transferring weight-bearing loads to the relatively unaffected lateral compartment in varus knees [3]. Osteotomy is a realignment procedure performed to prevent OA.

The majority of studies on varus knee osteotomy collected their data by self-assessment questionnaires [4]. Survival analyses were used to evaluate the clinical outcome of the surgery. These analyses indicated that osteotomy has an acceptable outcome for pain reduction in the short term; however, it deteriorates with time. Studies on the clinical outcome of osteotomy surgery have demonstrated satisfactory results for this surgery in the first five years. However, the outcomes for 10 and 15 years post-surgery have demonstrated poor results. These findings indicate the deterioration of results over time, although studies by Koshino et al. [5] and Akizuki et al. [6] have indicated high survival rates for HTO.

In another available and valuable method, gait analysis has been used to evaluate the outcome of HTO. This method uses inverse dynamics, force plate, and anthropometric data to calculate the forces and moments of joints. It is used to measure the functional outcome and indicate the forces of the knee. Unlike survival analysis and questionnaires that are dependent on patient reports, gait analysis is independent of these methods and can present functional results without patient involvement [4]. Different studies have used a variety of gait analyses to investigate the effects of surgery. Parameters used include the contact pressure [1,7–11], adduction moment [12–14], knee angle [15,16], knee moments in three planes [16–18], speed [16,17], knee kinematics [7], contact force [9,19], intra-articular ankle pressures [10], knee axial alignment [14,20], stability [21], and knee joint line orientation [22].

The majority of these studies are clinical-based without biomechanical insight into the surgical effects. Biomechanical studies using electronic sensors have been performed *in-vivo*; however, *in-vivo* measurements are invasive and harmful. Moreover, the variability of knee anatomy among the subjects and loading

* Corresponding author.
E-mail addresses: Badie-fateme@aut.ac.ir (F. Badie), katoozian@aut.ac.ir (H.R. Katouzian).

https://doi.org/10.1016/j.medengphy.2019.02.001
1350-4533/© 2019 Published by Elsevier Ltd on behalf of IPEM.

during functional tasks requires a subject-specific knee model, and kinetic and kinematic measurements.

According to the studies on HTO effects, the contact forces before and after surgery obtained by subject-specific knee anatomy and noninvasive measurements provide more reliable results.

The aim of the present study is to define a subject-specific three-dimensional (3D) multibody (MB) model of the knee. The MB model is obtained using the finite element (FE) method, according to the method proposed by Guess et al. [23]. The model includes bones (Tibia, Femur, and Fibula), cartilages (Tibia cartilage and Femur Cartilage), and menisci. This model is used to investigate the effect of osteotomy surgery on the contact forces of the cartilages and menisci during the stance phase of gait. It is assumed that osteotomy transfers the loading from the medial compartment of the knee to the lateral part. Using this MB model, it is possible to demonstrate the outcome of surgery during gait loading at a reasonable cost.

2. Materials and methods

2.1. Subject

A 20-year-old patient with varus alignment participated in this study. He was scheduled for a medial opening wedge HTO. The height and weight of the subject were 183 cm and 67 kg, respectively.

The information on the height and weight of the patient were used as demographic parameters for an inverse dynamic procedure.

The geometry of the knee was obtained by magnetic resonance images (MRIs) before and after surgery. The MRIs of the specimens were obtained with a 1.5 T clinical MRI scanner (SIEMENS) using a slice thickness of 3 mm. Manual segmentation of the images was performed using Mimics® (Materialise NV, Belgium). Then, the 3D model data in Mimics were exported as point clouds in the STL file format and imported into Geomagic Studio (Morrisville, NC). The point clouds were converted to surfaces and exported as a STEP-file in Geomagic Studio. This STEP-file was imported into CAD software CATIA (CATIA V5R21, Dassault Systems, France) as polylines.

The X-ray images of the knee joint before and after surgery indicated a correction of the knee angle (Fig. 1).

A 6-camera Vicon MX3 Motion Analysis System (Vicon, Oxford, UK) was used to collect kinematic data at a sampling rate of 100 Hz. Two force plates embedded into a 3-meter walkway (Kistler, Switzerland and AMTI, Watertown, MA, USA) were used to collect the kinetic data at a sampling rate of 400 Hz.

2.2. Computational models

A knee model was defined to investigate the effects of osteotomy on the cartilages. This model consisted of two parts: FE models and MB models. The FE and MB models were modified in Abaqus and Adams, respectively.

The FE and MB models included three parts: Menisci, Tibiofemoral (TF) joint, and Tibio-menisco-femoral (TMF) joint. These models were modified according to the models presented by Guess et al. [23]. The FE models were developed to obtain the parameters of the MB models.

In this model, it was necessary to determine the stiffness matrix of the menisci and the parameters of the cartilage-cartilage and cartilage-meniscus contact to define the knee model. To achieve this, first the FE model was defined, then, the parameters of the MB models were obtained by optimizing the force-displacement relationship of the FE and MB models. The FE models were defined before and after surgery, separately. Then, they were validated by previous studies.

Fig. 1. The X-ray of the knee, (a) before and (b) after surgery.

2.2.1. Menisci model

Finite element analysis. The geometry of the menisci was defined with the use of the MRI images. The menisci were considered as linearly elastic transversely isotropic materials. Young's modulus and Poisson's ratio in the symmetric plane were 20 MPa and 0.2, respectively; these values for the normal axis to the plane of isotropy are 150 MPa and 0.3, respectively. The density of the menisci was considered as 1100 kg/m^3 [24].

Multibody. The MB model of the meniscus was created by radial sectioning of its geometry. The mass properties of each section were obtained using its volume and a density of 1100 kg/m^3.

Field elements (a linear element through the use of a constant, orthotropic constitutive matrix, and orthotropic torsional spring) [25] were considered as the connecting parts of each meniscus. Eq. (1) presents the stiffness matrix:

$$\begin{bmatrix} F\theta \\ Fr \\ Fz \\ T\theta \\ Tr \\ Tz \end{bmatrix} = \begin{bmatrix} K_\theta & K_{\theta r} & K_{\theta z} & 0 & 0 & 0 \\ K_{\theta r} & K_r & K_{rz} & 0 & 0 & 0 \\ K_{\theta z} & K_{rz} & K_z & 0 & 0 & 0 \\ 0 & 0 & 0 & T_\theta & 0 & 0 \\ 0 & 0 & 0 & 0 & T_r & 0 \\ 0 & 0 & 0 & 0 & 0 & T_z \end{bmatrix} \begin{bmatrix} \theta \\ r \\ z \\ a \\ b \\ c \end{bmatrix} \quad (1)$$

where $F_{\theta,r,z}$ and $T_{\theta,r,z}$ are the translational and torsional forces between elements acting in the circumferential, radial, and axial directions, K_θ, K_r, K_z, $K_{\theta r}$, $K_{\theta z}$, and K_{rz}; T_θ, T_r, and T_z are the stiffness matrix parameters; θ, r, and z are relative translational displacements; and a, b, and c are relative rotational displacements.

Simulation. In the MB model for menisci, the sections of each meniscus were connected to a node by beam elements. In the FE models for menisci, the elements of the menisci were connected to that node via coupling (Fig. 2). The horn attachments of the menisci were fixed in all directions. A ramp force with the amplitude of 100 N in 1 s was applied to the reference nodes in the FE and MB models. The outputs of the two models were displaced by the reference nodes along the axes of the force as a function of time.

The purpose of this section was to obtain the stiffness parameters of the menisci using the FE model. To obtain the stiffness

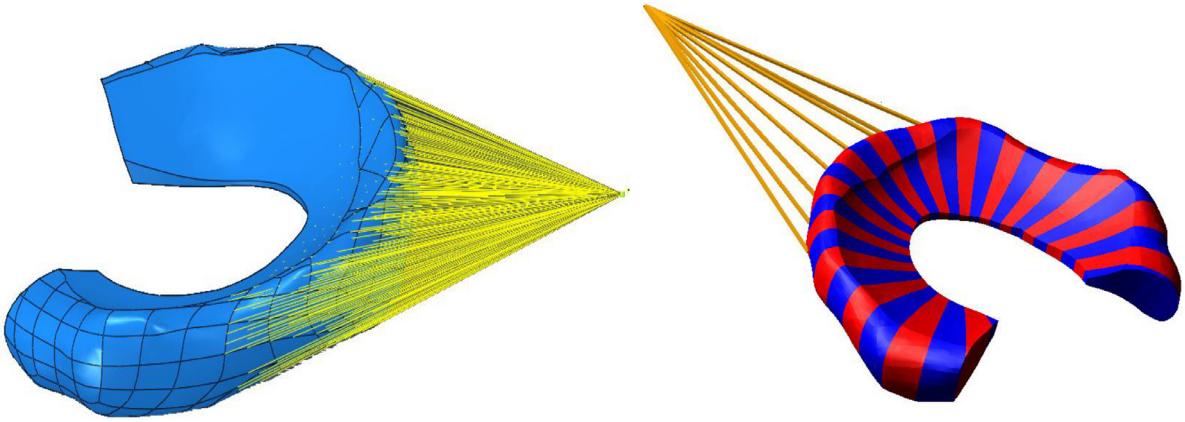

Fig. 2. The reference nodes are located where the force vectors are applied to the lateral surface of the meniscus.

parameters in the MB model of the menisci, it was necessary to minimize the displacement error between the FE and MB models. The root mean square (RMS) error was considered as an objective function and design of experiment (DOE) was used to obtain the stiffness parameters in the MB model.

DOE is a collection of procedures and statistical tools for planning experiments and analyzing the results.

In this study, DOE with a two-level fractional factorial design was considered as a screening algorithm. Thereafter, a two-level fractional factorial design was used to determine the statistically significant factors and a cubic model was used to obtain the minimum object function using a nonlinear model of significant factors. The correlation coefficient of determination ($R_{adj} > 0.9$, and $P < 0.005$) was used to ensure the validity of the results.

2.2.2. Tibio-femoral joint model

Finite element analysis. The TF joint consisted of the femur, tibia, and cartilages; the geometries were obtained from 3D MR images. The femur and tibia were assumed to be linear, elastic, and isotropic materials with Young's Modulus of 20 GPa and 18 GPa, respectively. Poisson's ratio of 0.2 and a density of 1600 kg/m^3 were considered for the bones. The cartilages were defined as linear, elastic, and isotropic materials with Young's modulus of 15 MPa and Poisson's ratio of 0.475. The density of the cartilages was considered as 1000 kg/m^3 [23].

The anterior cruciate ligament and medial collateral ligament were represented by four one-dimensional (1D) linear springs with a total stiffness of 1600 N/mm [23]. The lateral collateral ligament (LCL) and posterior cruciate ligament (PCL) are slack under compressive loading at zero degrees of flexion and do not influence joint contact behavior [24]. Therefore, these ligaments were not included in the model. The insertion sites for the ligaments were obtained from the MRI images.

All degrees of freedom of the femur were constrained and the tibia was constrained to flexion/extension.

Multibody. The TF joint model by Adams includes the tibia, femur, and cartilage geometries. The compliant contact force model of Hertz was used to determine the TF cartilage contact parameters. In Hertz's model, the normal contact force is defined as:

$$F = k\delta^n \tag{2}$$

where k and n are the stiffness coefficient and power exponent, respectively. In this model, using the elastostatic theory, the contact force is computed from the material and geometric properties. The Hertz's model is used for contacts involving elastic deformation, and the dissipation of energy is not included in this model. To model a compliant contact for cartilage, Hertz's contact formulation with the addition of a linear spring damper to dissipate the energy, as presented in Eq. (3), was employed to model the interaction between the tibial cartilage and femoral cartilage (27).

$$F_{TF} = \mathrm{k_c}\delta^{\mathrm{exp_c}} + \mathrm{B_c}(\delta)\dot{\delta} \tag{3}$$

where δ is the penetration degree and $\dot{\delta}$ is defined as the rate of the interpenetration at the contact point. k_c, exp_c, and B_c are parameters defining the contact between TF articulating cartilages.

Because of the difficulty in defining the contact parameters, stiffness and damping coefficients were considered as design variables in an optimization process to fit the output of the MB and FE models.

Simulation. In both the FE and MB-TF models, the following boundary condition and loading were applied. The proximal femur was constrained in all directions and the tibia flexion-extension rotation was fixed. A compressive axial load that linearly increased from zero to body weight (700 N) in 1 s was then applied to the distal tibia [24].

The contact parameters were obtained at this level. In the TF joint model, the RMS of the transitional displacement error in three directions between the FE and MB models was considered as an objective function.

The design variables in this section were contact parameters. Similar to the menisci, DOE was used to obtain the optimal match between the FE and MB models of the TF joint. The DOE included a two-level full factorial design and a higher order cubic model.

2.2.3. Tibio-menisco-femoral joint model

Finite element. The TMF model was developed by adding the menisci models to the TF model. Each meniscus was connected to the tibia via four 1D linear springs. The stiffness of each spring was 1000 N/mm [23]. During simulation in the TF and TMF models, all degrees of freedom of the femur were constrained and the tibia was constrained in flexion/extension.

Multibody. The TMF model was obtained by adding menisci to the TF model. The compliant contact of cartilages and each meniscus element was simulated in the 3D MB TMF joint model as explained in the TF section. Eq. (4) indicates this compliant contact:

$$F_{TMF} = \mathrm{k_m}\delta^{\mathrm{exp_m}} + \mathrm{B_m}(\delta)\dot{\delta} \tag{4}$$

where $\mathrm{k_m}$, $\mathrm{exp_m}$, and $\mathrm{B_m}$ are parameters defining the compliant contact between the meniscus and cartilage. The stiffness and damping coefficients were considered as design variables.

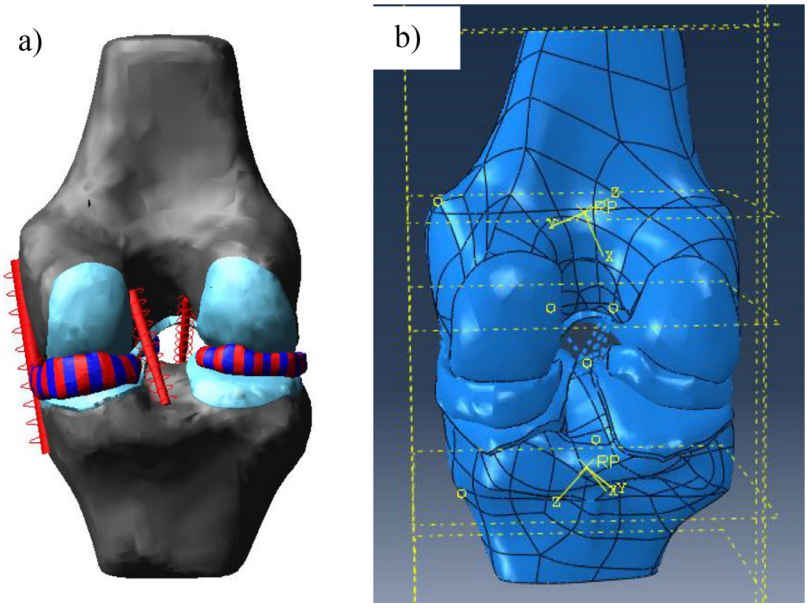

Fig. 3. The geometric model of knee in the Multibody (a) and Finite element (b) software.

Simulation. The loading and boundary conditions were defined the same as those for the TF model. However, the output of the TMF model was axial displacement. The final MB TMF model was defined as the knee joint. In this model, the parameters from earlier studies were used; the stiffness parameters of the menisci and parameters of the cartilage-cartilage and cartilage-meniscus contact were used to develop a subject-specific knee joint.

The ACL, MCL, LCL, and PCL were considered as 1D nonlinear springs. The force-displacement curves of the ligaments were defined by the nonlinear splines that form the nonlinear "toe" region. The ligament force was defined as a function of strain, length of ligament, and zero-load length.

$$f = \begin{cases} \frac{1}{4}k\varepsilon^2/\varepsilon_1 & 0 \le \varepsilon \le 2\varepsilon_1 \\ k(\varepsilon - \varepsilon_1) & \varepsilon > 2\varepsilon_1 \\ 0 & \varepsilon < 0 \end{cases}$$

$$\varepsilon = \left(\frac{l - l_0}{l_0}\right) \tag{5}$$

where k is a stiffness parameter and ε_1 is a spring parameter that is comprised of the nonlinear "toe" region that was assumed to be 0.03. The stiffness for each ligament bundle was obtained from Wismans et al. [26] and Blankevoort et al. [27].

Each meniscus was attached to the tibia plateau via linear 1D springs with a stiffness of 1000 N/mm as horn attachments.

The transverse ligament was a 1D spring with a stiffness of 200 N/mm. A parallel damper with a damping coefficient of 0.5 Ns/mm was included for each horn attachment and ligament spring. This procedure was used to develop the knee model before and after the osteotomy surgery.

The images of the two models are presented in Fig. 3.

2.2.4. Inverse dynamics

An inverse dynamics analysis was then performed to obtain the knee reaction forces and moments during the stance phase of gait. Although the gait analysis was performed three times on the patient before and after surgery, the data input into the MB model of the knee were provided by using the average of these three trials.

The loading applied to the model were the axial forces F_y, anterior/posterior force F_x, medial-lateral force F_z, varus/valgus moment M_x and internal/external rotation moment M_y.

Table 1
Maximum displacement of the load application point in menisci.

			Lateral meniscus	Medial meniscus
Maximum displacement (mm)	FE	Before surgery	0.85	1.77
		After surgery	0.71	0.69
	MB	Before surgery	1.61	2.09
		After surgery	1.55	0.95
	Guess et al. [23]		1.87	1.95

The loading on the knee was defined as the net forces and moments. The net loading was determined by the inverse dynamics and was imported as splines in the model.

The loads considered in this study were defined using inverse dynamics. Inverse dynamics analysis is commonly used to estimate the net loads at a joint during motion. The net loads (forces and moments) acting at a joint were generated by a combination of muscle, ligament, and joint contact forces. In the net joint, the moment contribution of the different muscles to the net moment could not be determined.

The primary functional role of the patella is knee extension. The patella increases the angle at which the quadriceps tendon functions. Consequently, the leverage of the tendon exerted on the femur increases. In this study, neither the patella nor the contributions of the muscles were considered in the model.

3. Results

3.1. Menisci

The maximum displacement of the load application point in the MB and FE models of the menisci was obtained and the results were compared with the results reported by Guess et al. [23] (Table 1).

According to the findings, the maximum displacement after surgery in the medial and lateral menisci was reduced. In the medial meniscus, variations of the results were approximately 1.1 mm in the MB and FE models. The maximum displacements decreased by approximately 0.1 mm in the lateral menisci in the FE and MB models. The differences between our results and the

Table 2
Maximum displacement of the load application point in TM.

			X	Y	Z
Maximum displacement (mm)	Finite element	Before	0.80	0.45	2.29
		After	1.82	0.91	2.20
	Guess et al. [23]		2.75	1.50	3.80

Table 3
Maximal contact pressure.

		Before surgery	After surgery	Zheng [1]
Maximal contact pressure (MPa)	Menisci	12.60	3.10	3.20
	Femoral cartilage	3.16	2.13	1.88
	Tibial cartilage	4.77	3.46	3.06

Table 4
Maximal contact forces.

	Before surgery	After surgery
Medial contact (N)	1224.94	1017.39
Lateral contact (N)	886.51	900.10
Total contact (N)	2101.69	1888.58

results reported by Guess et al. [23] range from 0.1 to 1.0 mm, which can be considered negligible.

3.2. Tibio-femoral joint

The FE model of the TF joint was defined as previously explained and the maximum displacements of the reference points were obtained in three directions (Table 2). These displacements are in millimeters.

The y-axis was aligned along the axial direction whereas the *z*- and *x*-axes were aligned in the medial-lateral and anterior-posterior directions. The results of the simulation according to the model implemented by Guess et al. [23] are presented in Table 2.

3.3. Tibio-menisco-femoral joint

The FE TMF model was validated. The maximal contact pressure in the cartilages and menisci of the FE model of the TMF joint was compared with those reported by Zheng [1] (Table 3).

These models were used to obtain the final knee model. The knee model was defined using the stiffness matrix, cartilage-cartilage, and cartilage-meniscus compliant contact that were obtained in previous sections. This model was a subject-specific MB model. Thereafter, forces and moments developed during the stance phase of gait were calculated using inverse dynamics. These forces and moments were also subject-specific.

The loading was applied to the subject-specific knee model and contact forces were obtained. The following figures display the results of the contact forces. Fig. 4 presents the contact forces before and after surgery. Each figure includes the medial and lateral contact forces.

Using the contact forces obtained for the lateral and medial parts, the total contact force was estimated for before and after surgery (Fig. 5).

It is believed that osteotomy shifts the medial loading axis to the lateral side. To investigate this hypothesis, the forces and moments applied to the knee model and the contact forces on the medial and lateral compartments before and after surgery were obtained. Moreover, the total contact force on the cartilages was measured. Osteotomy modifies the geometry of the knee and leads to a correction of the gait. The hypothesis is that the total contact force on the soft tissues also decreases after surgery. Table 4 presents the results of the maximal contact forces. The maximal and average loading reported by Guess et al. [23], Zhao et al. [28], and Damm et al. [29] are presented in Table 5 for comparison.

Table 5
Maximal and average contact force.

	Maximal loading (BW)	Average loading (BW)
Before surgery	2.76	2.29
After surgery	2.48	2.26
Guess et al. [23]	5.30	2.70
Damm et al. [29]	2.20	–
Damm et al. [30]	2.57	–

Other parts that influence the transfer of forces are the menisci. An understanding of the contact forces that develop on the menisci is important for investigating the impact of the surgery. In this study, to demonstrate the properties of the menisci, they were divided into smaller parts. Then, these parts were connected with the field elements.

Fig. 6 presents the contact force between the tibial cartilage and menisci. These diagrams include four parts, medial, lateral, before, and after surgery. The diagrams are 3D and the axes are time in seconds, force in Newtons, and the number of elements of the menisci.

4. Discussion

The innovation of this study was the development of a subject-specific knee model for a patient with varus knee alignment. To predict the surgical influences on the patient, noninvasive measurements were used. In a study on a cadaver knee, using the gait analysis of another person is necessary; in this study, the gait analysis of the live subject was used.

Earlier studies on contact forces in osteotomy surgery used invasive measurements and cadaver knees; the purpose of this study was to define a subject-specific knee model using noninvasive data. This model can be used to evaluate the surgical effects on the knee. Different parameters were investigated during the development of the knee model and their results were examined to validate and compare with similar studies and models. They are presented below. Upon comparison, our findings were similar to the results of the other studies.

4.1. Menisci

The first step in defining the knee model was the development of the FE and MB models of the menisci. The variation of the results of this model could be due to the changes in the knee geometry upon surgery. The properties of soft tissues were defined according to their geometries. Whereas the translation of the bones in this surgery led to variations of the soft tissue's geometry, the behavior where the menisci changed was predictable. At this level, to validate the menisci model, the loading and boundary conditions of the menisci model presented by Guess et al. were used [23]. The degree of correspondence between our results and those reported by Guess et al. extends the confidence in the results of the present study [23].

4.2. Tibio-femoral joint

The results of this section were presented for comparison with the results of Guess et al. [23]. The differences ranged from 0.1 to 1.0 mm, which can be considered negligible. Hence, they validate the results of the FE model [23]. As evidence, the differences observed between the results in three directions were minimal. Thus, based on the subject's variation in loading and gait, these differences are admissible.

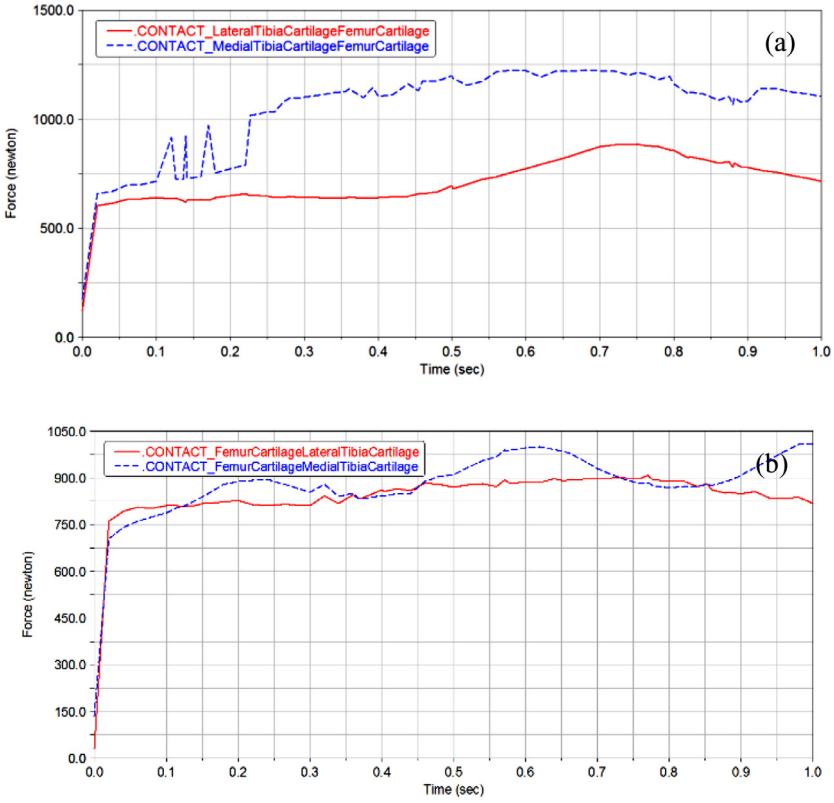

Fig. 4. Medial and lateral contact force, (a) Before, (b) After.

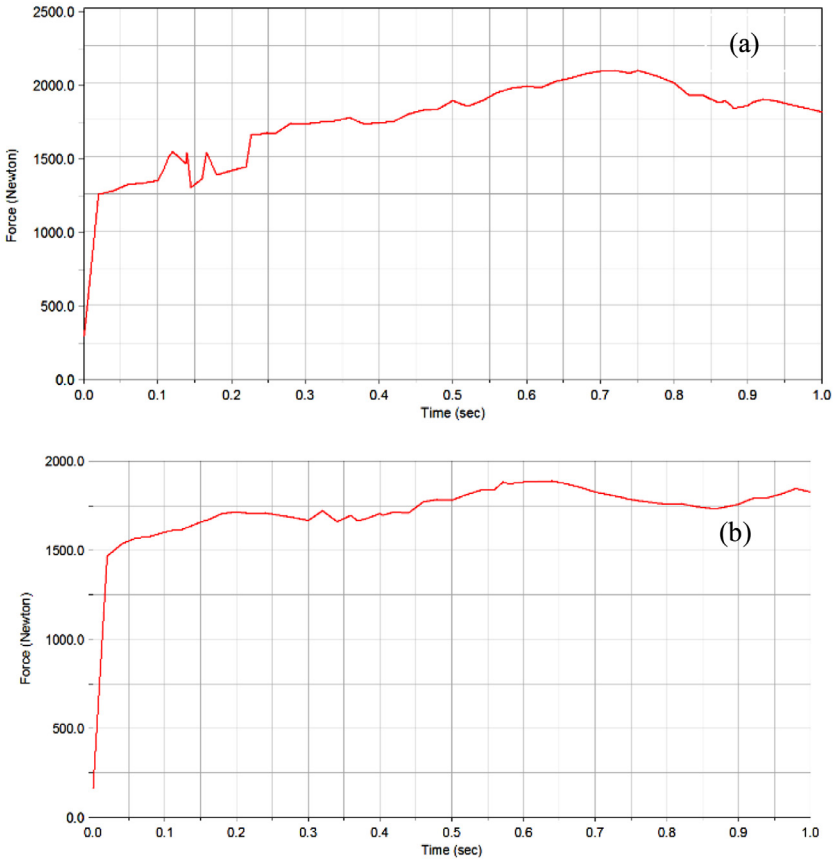

Fig. 5. Total contact force, (a) Before, and (b) After surgery.

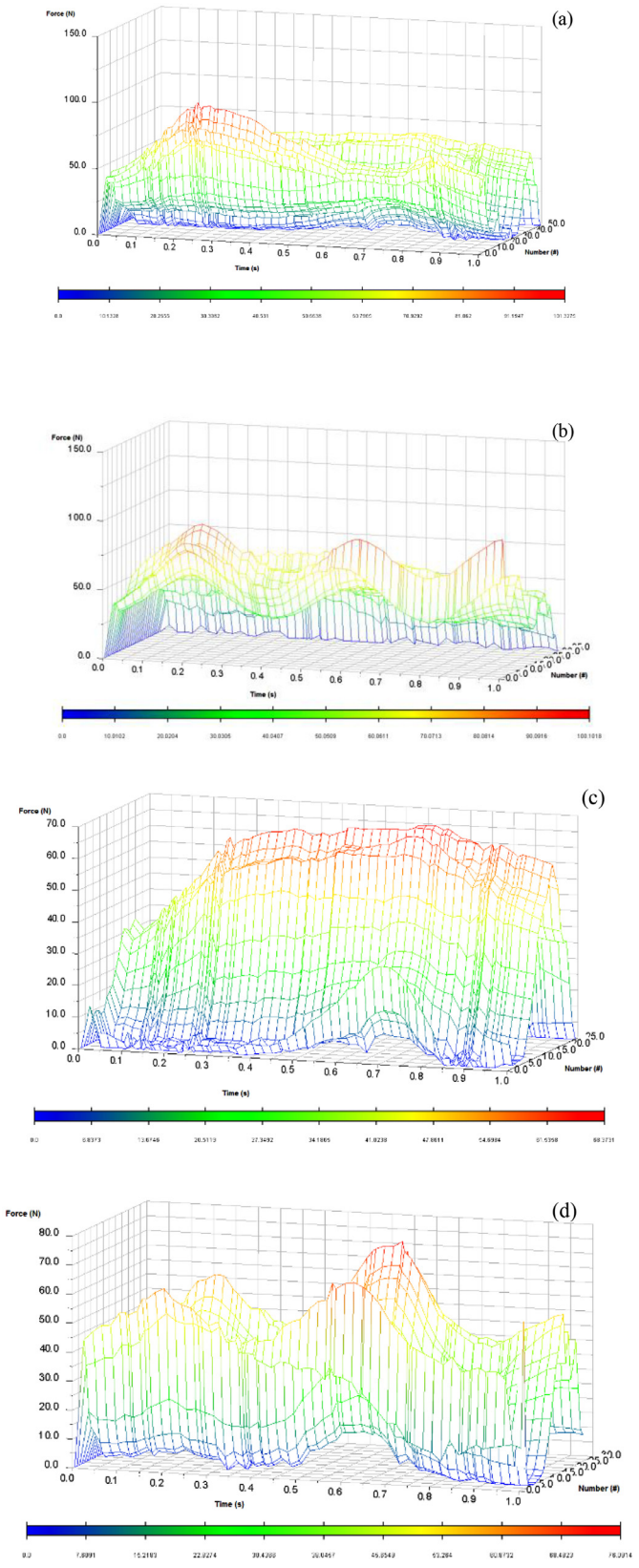

Fig. 6. Contact force between tibial cartilage and menisci, (a) lateral menisci before surgery, (b) lateral menisci after surgery, (c) Medial menisci before surgery, (d) Medial menisci after surgery.

4.3. Tibio-menisco-femoral joint

The TMF joint was simulated by attaching the menisci to the TF joint. In the results section, the maximal contact pressure before and after surgery was calculated. This simulation was developed by Zheng [1]. The applied force in the Zheng's model was 740 N and the ligaments were presented using the geometry model [1]. In our study, the force was 700 N and the ligaments were defined as linear springs. Based on these differences, our results are consistent with those of other studies.

The final knee model was developed using the MB TMF model that was defined and validated; however, in the knee model, the ligaments were presented as nonlinear springs.

As expected, after surgery, the medial and total contact decreased and the lateral contact force increased. The variation of medial and lateral contact decreased after surgery. The maximal and average contact forces during the stance phase of gait reported by Guess et al. [23], Zhao et al. [28], and Damm et al. [29] are in agreement with our results.

The patient in this study suffered from varus knee; however, the knee models employed by Guess et al. [23], Zhao et al. [28], and Damm et al. [29] had normal alignments, which is the reason of the differences in results.

The important part considered in this model was the menisci. We investigated the influence of the osteotomy surgery on the menisci by measuring the contact forces. The contact forces on the menisci before and after surgery had no significant variation. Therefore, osteotomy had no effect on the menisci.

The purpose of an HTO is to transfer the load from the medial to the lateral compartment. In this study, a 3D subject-specific MB analysis was performed noninvasively to investigate the effect of HTO on the contact forces at the cartilages and menisci in the knee joint. The MB model involved in the present study was defined with the use of subject-specific MR images and an FE model. To validate this model, the contact forces at the cartilage and meniscus were compared with the literature under identical loading conditions. The contact force at the medial cartilage decreased as the loading axis shifted to the lateral compartment. The results confirm the hypothesis of the present study.

The model applied in this study can be used as a preoperative tool to assist surgeons predict the outcome of HTO surgery. Further, because of the low computational cost, it is a suitable tool for analyzing complicated ambulation.

5. Conclusion

In this study, a subject-specific 3D MB model of the knee was developed to evaluate the effect of osteotomy on cartilages and menisci during the stance phase of gait. First, the geometries of the bones, cartilages, and menisci were determined using the MRIs of a patient with varus alignment. Then, the parameters for the stiffness matrices and compliant contact models of the TMF articulations were obtained using FE solutions. The results indicated that the contact force at the medial cartilage decreases when the load-bearing axis is transferred to the lateral parts. According to the results, it was concluded that this subject-specific noninvasive analysis of contact force could be an efficient preoperative assessment tool for predicting the effects of HTO and shifting the load-bearing axis on the soft tissues of the knee.

6. Limitations

This study focused only on the stance phase of a walking cycle. Further, only the parameters of one subject were used to develop the model. Future studies should be performed on a number

of cases to improve the validity of the findings. Moreover, the parameters of the soft tissues in the MB model were obtained based only on FE solutions, and muscles were not included in the study. Developing subject-specific musculoskeletal models from detailed MRI datasets and extracting soft tissue parameters directly from experimental measurements could improve the prediction accuracy. Furthermore, applying muscle forces and muscle activation models could improve the prediction of the joint forces.

Funding

This research did not receive any specific grant from funding agencies in the public, commercial, or not-for-profit sectors.

Conflict of interest

None

Ethical approval

The experimental procedure was approved by the ethics committee of the Amirkabir University of Technology, Iran.

Referrences

[1] Zheng K. The effect of high tibial osteotomy correction angle on cartilage and meniscus loading using finite element analysis; 2014.
[2] Amis AA. Biomechanics of high tibial osteotomy. Knee Surg Sports Traumatol Arthrosc 2013;21:197–205.
[3] Sischek EL, Birmingham TB, Leitch KM, Martin R, Willits K, Giffin JR. Staged medial opening wedge high tibial osteotomy for bilateral varus gonarthrosis: biomechanical and clinical outcomes. Knee Surg Sports Traumatol Arthrosc 2014;22:2672–81.
[4] Ornetti P, Maillefert JF, Laroche D, Morisset C, Dougados M, Gossec L. Gait analysis as a quantifiable outcome measure in hip or knee osteoarthritis: a systematic review. Joint Bone Spine 2010;77:421–5.
[5] Koshino T, Murase T, Saito T. Medial opening-wedge high tibial osteotomy with use of porous hydroxyapatite to treat medial compartment osteoarthritis of the knee. J Bone Joint Surg Am 2003;85:78–85.
[6] Akizuki S, Shibakawa A, Takizawa T, Yamazaki I, Horiuchi H. The long-term outcome of high tibial osteotomy: a ten-to 20-year follow-up. J Bone Joint Surg Br 2008;90:592–6.
[7] Agneskirchner JD, Hurschler C, Stukenborg-Colsman C, Imhoff AB, Lobenhoffer P. Effect of high tibial flexion osteotomy on cartilage pressure and joint kinematics: a biomechanical study in human cadaveric knees. Winner of the AGA-DonJoy Award 2004. Arch Orthop Trauma Surg 2004;124:575–84.
[8] Blecha LD, Zambelli PY, Ramaniraka NA, Bourban PE, Manson JA, Pioletti DP. How plate positioning impacts the biomechanics of the open wedge tibial osteotomy; a finite element analysis. Comput Methods Biomech Biomed Eng 2005;8:307–13.
[9] Mootanah R, Imhauser C, Reisse F, Carpanen D, Walker R, Koff M, et al. Development and validation of a computational model of the knee joint for the evaluation of surgical treatments for osteoarthritis. Comput Methods Biomech Biomed Eng 2014;17:1502–17.
[10] Suero EM, Sabbagh Y, Westphal R, Hawi N, Citak M, Wahl FM, et al. Effect of medial opening wedge high tibial osteotomy on intraarticular knee and ankle contact pressures. J Orthop Res 2015;33:598–604.
[11] Zhu Y, Chen JX, Xiao S, Mac Mahon EB. 3D knee modeling and biomechanical simulation. Comput Sci Eng 1999;1:82–7.
[12] Amis AA. Biomechanics of high tibial osteotomy. Knee Surg Sports Traumatol Arthrosc 2013;21:197–205.
[13] Birmingham TB, Giffin JR, Chesworth BM, Bryant DM, Litchfield RB, Willits K, et al. Medial opening wedge high tibial osteotomy: a prospective cohort study of gait, radiographic, and patient-reported outcomes. Arthritis Rheumatol 2009;61:648–57.
[14] Sischek EL, Birmingham TB, Leitch KM, Martin R, Willits K, Giffin JR. Staged medial opening wedge high tibial osteotomy for bilateral varus gonarthrosis: biomechanical and clinical outcomes. Knee Surg Sports Traumatol Arthrosc 2014;22:2672–81.
[15] Koshino T, Tsuchiya K. The effect of high tibial osteotomy on osteoarthritis of the knee. Int Orthop 1979;3:37–45.
[16] Lind M, McClelland J, Wittwer JE, Whitehead TS, Feller JA, Webster KE. Gait analysis of walking before and after medial opening wedge high tibial osteotomy. Knee Surg Sports Traumatol Arthrosc 2013;21:74–81.
[17] Leitch KM, Birmingham TB, Dunning CE, Giffin JR. Medial opening wedge high tibial osteotomy alters knee moments in multiple planes during walking and stair ascent. Gait Posture 2015;42:165–71.
[18] Marriott K, Birmingham T, Giffin R, Jones I. Gait biomechanics pre and post combined high tibial osteotomy and acl reconstruction. Osteoarthr Cartil 2014;22:S112–S1S3.
[19] Fregly BJ, D'Lima DD, Colwell CW. Effective gait patterns for offloading the medial compartment of the knee. J Orthop Res 2009;27:1016–21.
[20] Babis GC, An K-N, Chao EY, Larson DR, Rand JA, Sim FH. Upper tibia osteotomy: long term results—realignment analysis using OASIS computer software. J Orthop Sci 2008;13:328–34.
[21] De Albornoz PM, Leyes M, Forriol F, Del Buono A, Maffulli N. Opening wedge high tibial osteotomy: plate position and biomechanics of the medial tibial plateau. Knee Surg Sports Traumatol Arthrosc 2014;22:2641–7.
[22] Lee K, Chang C, Park M, Kang S-B, Kim T, Chung C. Changes of knee joint and ankle joint orientations after high tibial osteotomy. Osteoarthr Cartil 2015;23:232–8.
[23] Guess TM, Thiagarajan G, Kia M, Mishra M. A subject specific multibody model of the knee with menisci. Med Eng Phys 2010;32:505–15.
[24] Donahue TLH, Hull ML, Rashid MM, Jacobs CR. A finite element model of the human knee joint for the study of tibio-femoral contact. J Biomech Eng 2002;124:273–80.
[25] Bauchau OA. Flexible multibody dynamics. Springer Science & Business Media; 2010.
[26] Wismans J, Veldpaus F, Janssen J, Huson A, Struben P. A three-dimensional mathematical model of the knee-joint. J Biomech 1980;13:677–85.
[27] Blankevoort L, Kuiper J, Huiskes R, Grootenboer H. Articular contact in a three-dimensional model of the knee. J Biomech 1991;24:1019–31.
[28] Zhao D, Banks SA, D'Lima DD, Colwell CW, Fregly BJ. In vivo medial and lateral tibial loads during dynamic and high flexion activities. J Orthop Res 2007;25:593–602.
[29] Damm P, Kutzner I, Bergmann G, Rohlmann A, Schmidt H. Comparison of in vivo measured loads in knee, hip and spinal implants during level walking. J Biomech 2017;51:128–32.